# In Vitro Dissolution of Uniform Cobalt Oxide Particles by Human and Canine Alveolar Macrophages

W. G. Kreyling, J. J. Godleski, S. T. Kariya, R. M. Rose, and J. D. Brain

Projekt Inhalation, Gesellschaft für Strahlen- und Umweltforschung mbH München (GSF), Neuherberg, Federal Republic of Germany; Respiratory Biology Program, Harvard School of Public Health, Boston, Massachusetts; and Section on Pulmonary Disease, New England Deaconess Hospital, Boston, Massachusetts

Intracellular dissolution of inhaled particles is an important pathway of clearance of potentially toxic materials. To study this process, monolayers of human and canine alveolar macrophages (AM) were maintained alive and functional *in vitro* for more than 2 wk. Complete phagocytosis of moderately soluble, monodisperse <sup>57</sup>Co<sub>3</sub>O<sub>4</sub> test particles of four different sizes was obtained by optimizing the cell density of the monolayer and the particle-to-cell ratio. The fraction of the initial particle mass that was soluble increased over time when the particles were ingested by AM but remained constant when in culture medium alone. Smaller particle sizes had a faster characteristic intracellular dissolution rate constant than did larger particles.

The dissolution rates differed between AM obtained from two human volunteers as compared to those obtained from six mongrel dogs. These *in vitro* dissolution rates were very similar to *in vivo* translocation rates previously obtained from human and canine lung clearance studies after inhalation of the same or similar monodisperse, homogeneous  ${}^{57}\text{Co}_3\text{O}_4$  test particles. We believe an important clearance mechanism for inhaled aerosol particles deposited in the lungs can be simulated *in vitro* in a cell culture system.

Alveolar macrophages (AM) ingest particles deposited in the lungs. The role of these cells in phagocytosis and breakdown of bacteria and other organic materials is well known (1). Ingestion of inorganic particles by AM is also well defined (1), but subsequent AM-mediated clearance mechanisms remain controversial. A potentially important aspect, the dissolution of particles in AM with subsequent translocation of the dissolved material to the blood, has received less attention. Particle dissolution in the lungs has been recognized as an important clearance pathway (2–8), but the process was thought to be carried out extracellularly in the alveolar lining layer, airway mucus, or interstitial fluid. Thus, emphasis has been placed on models estimating dissolution rates of particles in simulated lung fluids or serum (3–7, 9–17).

Recent studies on beagle dogs showed that various forms of inhaled homogeneous cobalt oxide particles were cleared predominantly by dissolution of the particles in the lungs and subsequent translocation to blood (18, 19). The rate of disso-

Key Words: alveolar macrophages, cell culture, intracellular dissolution, monodisperse test particles;  $^{57}\text{Co}_3\text{O}_4$  particles

(Received in original form March 8, 1989 and in revised form November 1, 1989)

Address correspondence to: Dr. J. D. Brain, Harvard School of Public Health, Respiratory Biology Program, 665 Huntington Avenue I/1302, Boston, MA 02115.

Abbreviations: alveolar macrophage(s), AM; bronchoalveolar lavage, BAL; scanning electron microscope, SEM.

Am. J. Respir. Cell Mol. Biol. Vol. 2. pp. 413-422, 1990

lution of cobalt oxide in the lungs depended on the physicochemical properties of the particles such as size, density, specific surface area, and chemical composition. These particles dissolved negligibly in serum, lung fluid simulants, and saline solutions (20, 21). When pulmonary clearance of these particles was compared among different species, slightly different dissolution patterns for cobalt oxide (Co<sub>3</sub>O<sub>4</sub>) particles were found in humans, baboons, beagle dogs, guinea pigs, hamsters, mice, and three different strains of rats (22, 23). All of these data, however, were consistent with the hypothesis that dissolution of the particles occurred intracellularly in AM, because particles were shown to be phagocytized and because dissolution and translocation was far greater in vivo than in serum simulant solvents. Also, recent work has shown that cultured AM can dissolve some particles (24-30).

In the work reported here, the dissolution rates of monodisperse, chemically homogenous, radiolabeled <sup>57</sup>Co<sub>3</sub>O<sub>4</sub> particles of different sizes in cultured AM were determined. We also compared these rates to those found *in vivo* for the same particles and found them consistent. We believe an important clearance mechanism for particles deposited in the lungs, macrophage-mediated particle dissolution, can be simulated *in vitro*.

## Materials and Methods

57Co<sub>3</sub>O<sub>4</sub> Particles

To produce monodisperse  ${}^{57}\text{Co}_3\text{O}_4$  particles, a cobalt nitrate  $({}^{57}\text{Co}(\text{NO}_3)_2)$  aerosol was generated with a spinning-top aero-

sol generator, followed by thermal degradation at  $800^{\circ}$  C (21). The resulting spherical particles were porous, with a surface area 10 times larger than their calculated spherical area (31).  $\text{Co}_3\text{O}_4$  retains its chemical form and crystalline structure and does not decompose in ambient air. Four separate particle sizes (mean geometric diameter: 0.3, 0.7, 0.8, and 1.7  $\mu$ m) were used for these studies. All geometric standard deviations were about 1.1. The 0.8- $\mu$ m particles were originally made for a European interspecies comparison of lung clearance (22, 23, 32, 33).

# Alveolar Macrophages

Canine AM were obtained from six adult mongrel dogs of both sexes by bronchoalveolar lavage (BAL). Animals were anesthetized using intravenously administered thiamyl (2 mg/kg body weight; Parke Davis, Morris Plains, NJ); additional doses were given as necessary. BAL was performed with a fiberoptic bronchoscope (Model BF-IT; external diameter, 6 mm; Olympus Corp., New Hyde Park, NY). Under direct visualization, the bronchoscope was wedged gently in a subsegmental bronchus. Three aliquots of 15 ml sterile saline (Travenol Lab., Deerfield, IL) at room temperature were instilled via the instrument channel and then gently aspirated into a sterile suction trap. A total of 180 ml of saline was instilled per dog, divided equally among subsegmental bronchi in four different lobes. A differential count of 400 BAL cells was performed on Wright Giemsastained cytocentrifuge preparations (Cytospin 2; Shandon Southern Instruments, Sewickley, PA), using standard morphologic criteria (36). The remainder of the BAL was strained through four layers of sterile coarse cotton gauze to remove mucus and centrifuged at  $400 \times g$  for 10 min. The cell pellets were resuspended in medium RPMI 1640 (GIBCO, Grand Island, NY) supplemented with 2% penicillin/streptomycin (10<sup>4</sup> U/ml) and 5% FCS (GIBCO). Total cell counts were determined using a Coulter counter (Coulter Electronics Inc., Hialeah, FL) and confirmed with a hemocytometer.

Human AM were obtained from two healthy, adult, non-smoking male volunteers, 21 and 28 yr of age. Physical exam and spirometry were normal, and an informed consent form approved by the New England Deaconess Hospital Human Studies Committee was signed. BAL was carried out in a manner similar to that described above for the dogs, except that only intramuscularly administered atropine (0.4 mg) and topical lidocaine were used for local anesthesia. Three 50-ml aliquots of sterile saline were instilled into subsegmental bronchi in the right middle and lingula lobes (total of 300 ml instilled). Differential cell counts, centrifugation, and suspension of the cells in media were as described above.

For culture, canine or human BAL cells were transferred to RPMI 1640 medium with penicillin/streptomycin and 5% FCS. Aliquots were then placed in flat-bottom, 96-well plates at  $2 \times 10^4$  cells/well (Linbro cell culture plates; Flow Laboratories, McLean, VA). The plates were kept in a humidified incubator at 37° C with 95% air and 5% CO<sub>2</sub>. After an initial incubation of 2 to 4 h, the medium was changed to remove nonadherent cells. Aliquots of fresh RPMI 1640 media with antibiotics, 5% FCS, and  $^{57}\text{Co}_3\text{O}_4$  particles at a particle-to-cell ratio of 2:1 were then added. Adherent cells covered 5 to 10% of the surface area of the bottom of each

well. At least one plate containing cells without particles was used as a control. Also, for each particle size, plates containing particles, but no cells, were incubated.

To assure that all  ${}^{57}\text{Co}_3\text{O}_4$  particles had been ingested by AM, the cell culture plates for the 1.7- $\mu$ m particles were observed directly using an inverted light microscope at 200× magnification. Phagocytosis of the smaller particles was monitored in chamber slides (Lab-Tek) after incubation of cells and particles under the same conditions. After 3 d of incubation, fixed and Wright Giemsa-stained cells examined at  $400\times$  and  $1.000\times$  magnification showed that all particles were ingested. In preliminary studies, the cell concentration varied between  $5\times10^3$  and  $50\times10^3$  cells/well and the particle-to-cell ratio was between 0.5:1 and 20:1, in order to select the best conditions. Our criteria included cell maintenance during 2 wk of incubation and complete phagocytosis of the test particles within the first 2 to 3 d.

#### Quantitation of 57Co Dissolution

Measurements of the dissolved and the particulate fraction of 57Co were made at least five times over 2 wk. At each time point, for each particle size, media from six wells were removed and filtered with vacuum through a 0.22-µm membrane filter (diameter, 13 mm) to separate dissolved from particulate or cell-bound 57Co. To minimize wall losses, 100-ul samples were pipetted onto the filter supported on an open plastic filter holder (Millipore, Bedford, MA). The remaining cell monolayers were lysed by addition of 100 µl of 1% Triton X 100 to each well. After 15 min, cell lysates were removed and filtered through a separate membrane filter. Finally, the wells were thoroughly wiped with a cottontipped applicator stick. Filtrates of the samples contained the dissolved <sup>57</sup>Co fractions, while particulate material was found on filters and the cotton applicator. To determine differential counts of cell monolayers at different times, cells from two additional wells were gently removed by repeated pipetting. These cells were cytocentrifuged onto microscope slides and stained with Wright Giemsa.

The dissolved and particulate fractions of <sup>57</sup>Co were determined for each particle size by measuring radioactivities of all filtrates, filters, and cotton applicators separately using a Gamma counter (Packard Auto Gamma Scintillation Spectrometer). The control plates containing particles, but no cells, were similarly measured. Dissolution rates were calculated by approximating the dissolved <sup>57</sup>Co fractions at the various time points with an appropriate model as outlined later.

# In Vitro Cell Monitoring

At each time, all the cells in a strip across the well diameter were counted using an inverted light microscope (Leitz, New York). From these counts, the total number of cells per well was calculated. To evaluate the phagocytic function of the cells, 20 μl of 2-μm green fluorescent latex beads (Polysciences, Warrington, PA) were added to four wells of the control plate which contained AM but no Co<sub>3</sub>O<sub>4</sub> particles. Then the beads were gently mixed into the media of each well. The cell-to-bead ratio of 1:20 and the cell concentration at the well bottom (only 5 to 10% was covered with cells) were selected so that generally only single beads set-

tled onto cells. Settling of the beads on the well bottom was complete after 0.5 to 1 h of incubation, resulting in a uniform spatial distribution of beads on the bottom.

Twenty-four hours later, the distribution of beads was no longer uniform. Most of the beads were now cell-associated. Cells with two or more beads after 24 h were defined as phagocytic. The percentage of these cells and those with no or only one bead was determined by light microscopy. Comparisons of phagocytosis of latex between AM that initially had or had not ingested  ${}^{57}\text{Co}_3\text{O}_4$  particles were also carried out. The presence of ingested  ${}^{57}\text{Co}_3\text{O}_4$  particles had no effect on latex phagocytosis. Therefore, almost all phagocytosis measurements were made on AM controls without  ${}^{57}\text{Co}_3\text{O}_4$  particles. In a preliminary study, the cell concentration and phagocytic function of the cultured macrophages were followed for 6 wk.

To determine if binding of dissolved Co to protein had any effect on our analysis, protein was precipitated with TCA from filtered media as well as cell lysates and then separated by centrifugation. We also investigated extracellular particle dissolution by enzymes and/or other cell products released from the macrophages. In these studies, after 4 d of incubation, conditioned media was collected from wells containing AM and nonradioactive  $\text{Co}_3\text{O}_4$  particles or latex particles. After filtration of the harvested media, radioactively labeled  ${}^{57}\text{Co}_3\text{O}_4$  particles were added to the filtrate, incubated for 10 d, and assayed for dissolution.

The toxic effect of  $Co^{2+}$  ions in media at concentrations up to 1  $\mu$ g/ml on the AM *in vitro* was also investigated by morphologic appearance, as well as by sequential determinations of the cell concentration and phagocytic function.

Finally, to study the relationship between the cellular functions of phagocytosis and particle dissolution in AM, we changed the incubation temperature from 37° C to 20° C. Lower temperatures should slow down metabolic processes and provide a means to rank the temperature sensitivity of intracellular dissolution, cell survival, and phagocytic function. Two plates of AM from dogs 5 and 6 were prepared for 0.3- and 0.7-µm particles each. The temperature change was made in one plate 4 d after incubation in order to assure complete phagocytosis of the Co<sub>3</sub>O<sub>4</sub> particles; low temperature was then maintained for the next 10 d. During this time, intracellular dissolution, cell survival, and phagocytic function were compared with those obtained from cell cultures remaining at 37° C for the entire time.

# Modeling of Dissolution Kinetics

Dissolution of particulate matter depends upon chemical and physical properties of the solvent and the particles. The intrinsic solubility of a material is described by the dissolution rate constant k of this material in a certain solvent and the particle surface. In this study, for a given set of AM or media, we varied the physical particle parameters and kept the other variables constant. Hence, we derived a model that predicts dissolution rates as a function of particle properties. This model is applied to the measured dissolved fractions at the various time points, and thus the dissolution rates for the four particle sizes are calculated.

We assume that the rate of change of the remaining mass,

m, of a batch of particles is proportional to their surface area, S, (5, 6, 14, 15):

$$\frac{\mathrm{dm}}{\mathrm{dt}} = - k S \tag{1}$$

with k the dissolution rate constant.

The.  $^{57}\text{Co}_3\text{O}_4$  particles used in this study are monodisperse, spherically shaped, and structurally as well as chemically homogeneous (21, 31). However, because they are porous particles, dissolution could involve the inner as well as the outer surface area. To include this inner surface area, we assume that the ratio of the surface to mass, the specific surface area  $s_0 = S(t)/m(t)$ , remains constant over time. Then the fractional rate of change of mass is proportional to the remaining mass:

$$\frac{1}{m}\frac{dm}{dm} = -k \frac{S}{m} = -k s_0 \tag{2}$$

Therefore, the dissolved mass fraction at any time, t, is:

$$1 - \frac{m}{m_0} = 1 - e^{-k s_0 t}$$
 (3)

where m<sub>0</sub> is the initial mass of the particles.

The observed dissolution rates, K, of the four particle sizes should depend on the initial particle properties. These rates are the product of the dissolution rate constant k and the initial specific surface area  $s_0$ .

$$K = k s_0 (4)$$

In an earlier study (31), we found that the specific surface area of monodisperse, porous  $\text{Co}_3\text{O}_4$  particles of 1- $\mu$ m mean geometric diameter was 10 times larger than their spherical surface area. These particles were produced under the same conditions as the four batches used in this study.

The porosity of the  $\text{Co}_1\text{O}_4$  particles results from the rapid decomposition of the crystalline  $\text{Co}(\text{NO}_3)_2$  particles in the tube furnace. Because furnace temperature and aerosol flow velocity was the same for the production of all particles, the same specific surface area is assumed for all four particle sizes. Hence, the initial total specific surface area  $s_0$  is a function of the initial geometric particle diameter  $d_0$  of these spherical particles:

$$s_0 = \frac{10 \pi d_0^2}{\rho \pi/6 d_0^3} = \frac{60}{\rho d_0}$$
 (5)

The density of bulk  $\text{Co}_3\text{O}_4$  is  $\rho_0 = 6.05 \text{ g cm}^{-1}$ , but the density of these porous  $\text{Co}_3\text{O}_4$  particles is  $\rho = 3.0 \pm 0.5 \text{ g cm}^{-1}$  as determined from the mean geometric diameter measured by SEM and the aerodynamic median diameter measured by a Stöber aerosol centrifuge (21, 31).

#### Results

# Cells Recovered from BAL

Parameters of the canine BAL are given in Table 1. Human BAL cells numbered more than 10<sup>7</sup> and were at least 90% macrophages by differential counts.

Adherent cells that remained after the media was changed

TABLE 1

Recovery of the lavage fluid and total and differential cell counts obtained from the BAL from six dogs\*

| Volume of recovered lavage   |                |
|------------------------------|----------------|
| fluid (%)                    | $75 \pm 6$     |
| Total cells recovered (×106) | $22 \pm 8$     |
| Differential cell count (%)  |                |
| Macrophages                  | $74.7 \pm 6.1$ |
| Neutrophils                  | $7.4 \pm 2.8$  |
| Lymphocytes                  | $10.3 \pm 3.0$ |
| Eosinophils                  | $5.7 \pm 3.4$  |
| Mast cells                   | $1.2 \pm 0.9$  |
| Epithelial cells             | $0.7 \pm 0.9$  |
|                              |                |

<sup>\*</sup> Values are expressed as mean ± SD.

were always more than 95% AM. Monitoring of monolayer cultures with an inverted light microscope revealed that about 20 to 30% of the macrophages were lost during the first 2 wk of incubation. Figure 1a shows cell concentration in a control plate over a 4-wk period.

Approximately 85% of the AM in the control plates were capable of ingesting latex beads on the second and fourth day of incubation. After 2 wk of incubation, 60 to 70% of the cells still ingested the beads. Figure 1b shows the phagocytic function over a 4-wk period. Cell movement on the bottom of the wells was observed to be continuous, and the cells phagocytized free <sup>57</sup>Co<sub>3</sub>O<sub>4</sub> particles and cell debris. All par-

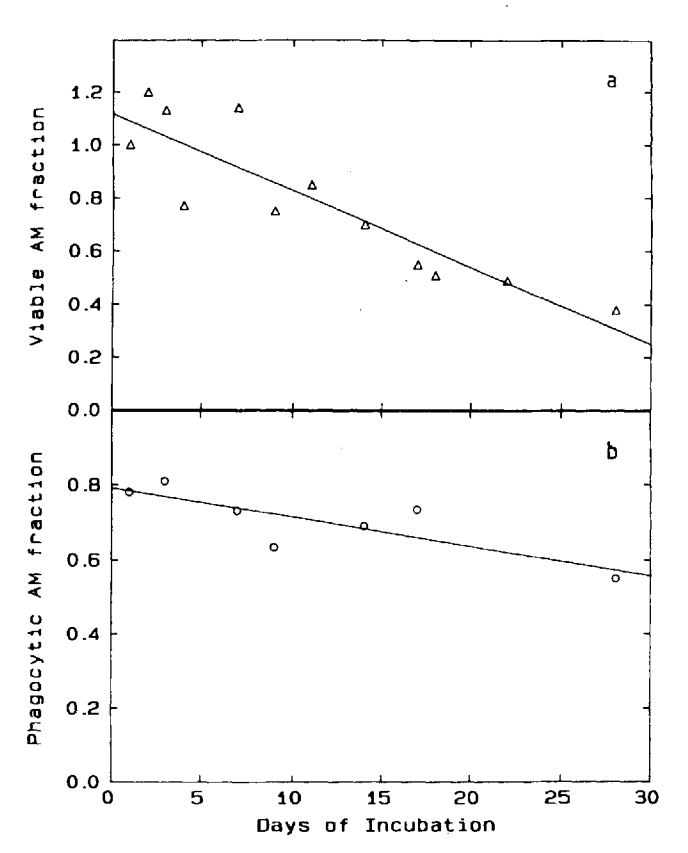


Figure 1. a. Concentration of viable canine alveolar macrophages (AM) normalized to the initial concentration in the wells. b. Fraction of cultured viable canine AM that phagocytized particles.

ticles were ingested within 2 to 3 d. At this time, the macrophages covered 5 to 10% of the well bottom and the particle-to-cell ratio was 2:1. Cobalt ion concentrations up to 1  $\mu$ g/ml in media affected neither AM concentrations, morphologic appearance, nor phagocytic function over a 2-wk period.

#### Particle Dissolution in Media

The fraction of Co that was soluble in particle-media suspensions without cells increased during the first 6 to 10 h after incubation but then remained constant throughout the entire 2 wk (Figure 2). Moreover, the dissolved Co fraction in media only was very small and characteristic for each particle size. The smaller the particles, the greater the dissolved fraction: 0.002, 0.007, 0.010, and 0.045 of the initial particle mass became solubilized for 1.7-, 0.8-, 0.7-, and 0.3- $\mu$ m particles, respectively. The addition of FBS to the medium had no effect on dissolution of the particles.

When media were changed after the first day, dissolved fractions were negligible at subsequent determinations, thereby indicating that the initial increase in the dissolved Co fraction reflected particle leaching of soluble Co rather than saturation of Co in the media. This leaching effect could be reduced significantly by washing the particles for 24 h prior to incubation.

#### Intracellular Dissolution of <sup>57</sup>Co<sub>3</sub>O<sub>4</sub> Particles

In Figures 2 and 3, the dissolved fractions obtained from AM of each dog are averaged for each time point and plotted with standard deviations. Similarly, the dissolved fractions for particles in media only are shown in Figure 2. The dissolved fraction in the latter remained constant during 2 wk, whereas the dissolved fractions of <sup>57</sup>Co by AM increased with time (Figure 2). The rate of dissolution was much faster for smaller particles than for larger particles. After 2 wk *in vitro*, 50%, 5%, 3%, and 2% of the initial particle mass was dissolved for 0.3-, 0.7-, 0.8-, and 1.7-µm particles, respectively.

In Figure 3, we distinguish the dissolved Co fraction in the cell culture supernates versus the cell lysates for the four different particle sizes. Most of the dissolved <sup>57</sup>Co appears in the supernates. In contrast to the increasing dissolved fraction in the AM culture supernates, the dissolved fractions recovered from the cell lysates were small and remained constant throughout the 2 wk. The mean dissolved Co fractions of the initial particle mass for all cell lysates are listed in Table 2 for all human and canine AM and all particles. Although the particles are clearly dissolved intracellularly, the dissolved Co is released into the media.

# Assessment of the Dissolution Model

In the application of the model for intracellular particle dissolution, particle-leaching fractions, as determined in the cell-free control plates, were subtracted from the dissolved fractions obtained from the AM cultures. From these data, mean dissolution rates K and standard deviations were calculated for each set of AM and each particle size using Equation 3. To test the constancy of the dissolution rate within the 2 wk of incubation, dissolution rates were calculated for: (1) the total period of incubation; (2) the final period, excluding data from the first 6 d; and (3) the initial period, excluding data after day 10. The standard deviations of these three rates are given in Table 3 for all human and canine AM and all

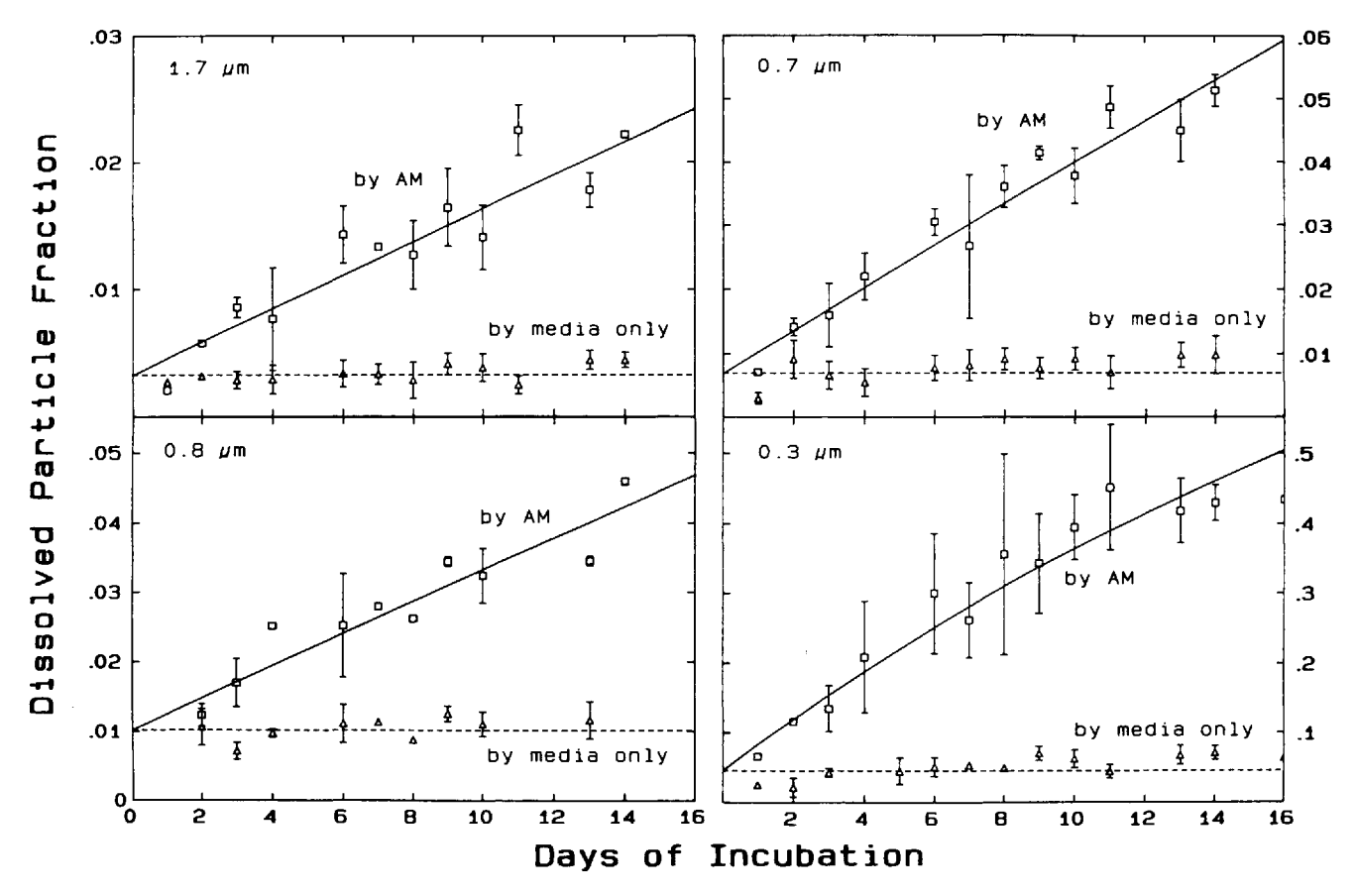


Figure 2. Mean dissolved <sup>57</sup>Co fractions of the initial <sup>57</sup>Co<sub>3</sub>O<sub>4</sub> particle mass averaged (with standard deviations) for each day of incubation. Data are presented for four different-sized particles phagocytized in canine AM or in cell-free media. Note that the vertical scales differ for the four particle sizes.

particles. (Each standard deviation was normalized to the mean of the three rates.)

The mean dissolution rate constant k as calculated by Equations 4 and 5 from all dog data is  $1.4 \pm 0.1 \times 10^{-8}$  g cm<sup>-2</sup> d<sup>-1</sup> for 0.7-, 0.8-, and 1.7- $\mu$ m particles. But for 0.3- $\mu$ m particles, the rate constant is  $7.2 \times 10^{-8}$  g cm<sup>-2</sup> d<sup>-1</sup>.

## Total and Intracellular In Vitro Dissolution Rates

In Table 4, total dissolution rates are calculated from the measured dissolved <sup>57</sup>Co fractions obtained at various times. These rates represent the combined effects of intracellular particle dissolution and particle-leaching. These rates will be compared later in the DISCUSSION section to *in vitro* translocation rates determined in previous lung clearance studies (19, 22, 23, 32–34). However, particle-leaching reflects a finite mass fraction on the particle surface which is dissolved within hours after the particle is immersed in the solvent. Later, particle-leaching is negligible as measured in the cell-free control plate, which is shown in Figure 2.

In order to derive the intracellular particle dissolution rate, the leaching fraction as determined simultaneously in the cell-free control plate was subtracted from each total dissolved fraction prior to fitting the data to an exponential function. These rates are given in Table 5. The standard deviations for all the rates are smaller than the corresponding rates in Table 4. This clearly indicates that the model for the

intracellular dissolution process improves when the term for extracellular dissolution with a larger dissolution rate is eliminated.

## Mechanisms of Particle Dissolution

The dissolved Co was not bound to intracellular or extracellular protein based on our protein precipitation studies. Therefore, Co must be dissolved in an ionic or complex state in the culture media.

Extracellular particle dissolution by enzymes and/or other cell products released from the macrophages did not occur. For all particle sizes, we observed no additional dissolution in conditioned media when compared to the initial leaching fraction seen in normal media. Therefore, dissolution was maintained only by intracellular dissolution processes and not by enzymes and/or other cell products released from AM.

When the incubation temperature was reduced from 37° C to 20° C after 4 d of incubation, the number of AM in culture and their phagocytic function did not change compared to the control cell cultures at 37° C. But no further dissolution occurred; the dissolved fractions remained constant from day 4 to 14 and did not increase when the cultures were incubated at 20° C. At the same time, particle dissolution in media without cells did not differ significantly for the two incubation temperatures. Comparisons of cultures incubated at 20° C and 37° C are shown in Figure 4 for 0.3- and 0.7-µm

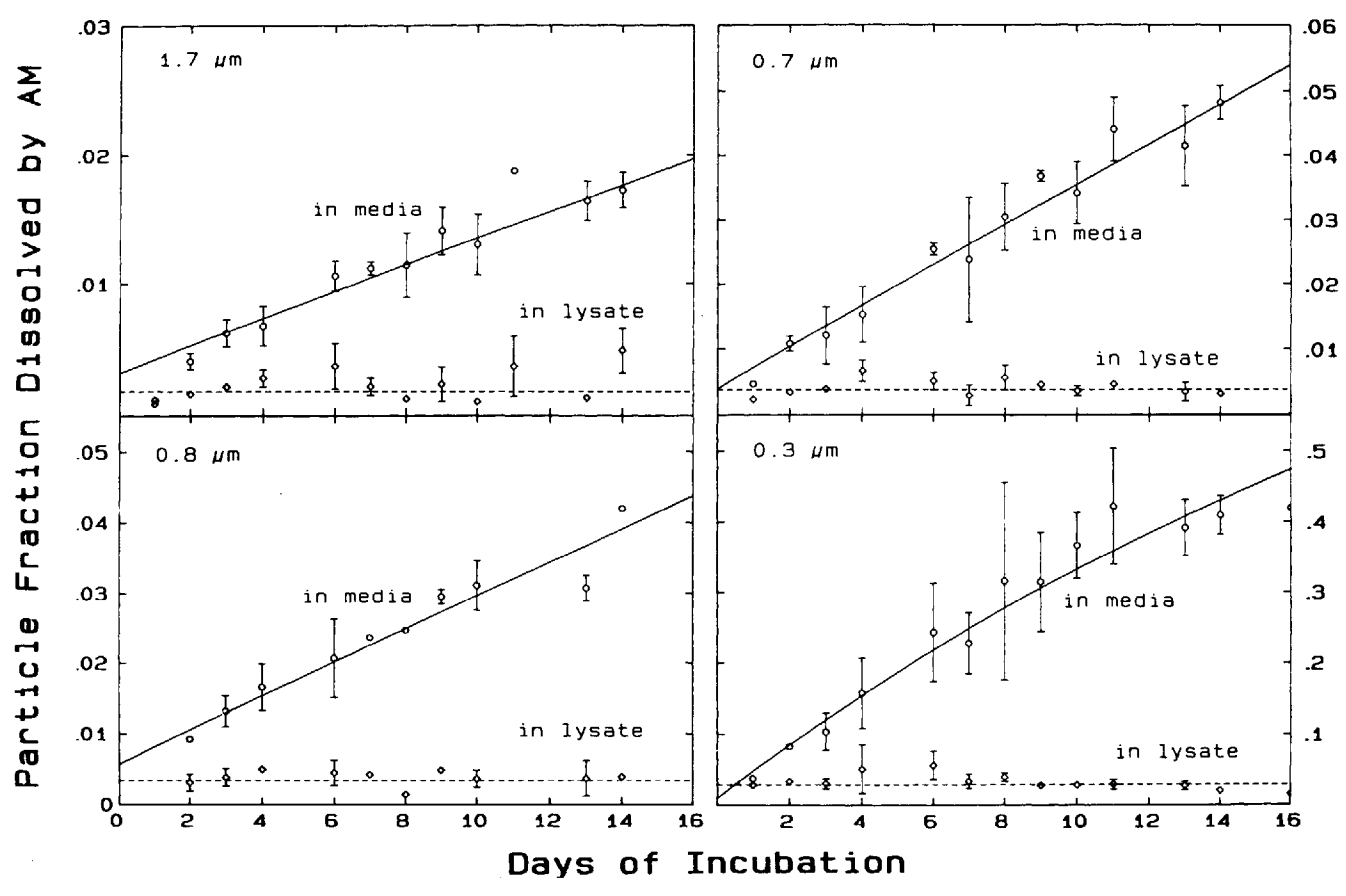


Figure 3. Mean dissolved <sup>57</sup>Co fractions of the initial <sup>57</sup>Co<sub>3</sub>O<sub>4</sub> particle mass averaged (with standard deviations) for each day of incubation. Data are presented for the dissolved fractions found in the well media and AM lysates for four different-sized particles phagocytized in canine AM or in the cell lysates (dissolved <sup>57</sup>Co remaining intracellularly). Note that the vertical scales differ for the four particle sizes.

particles. Although phagocytic ability of the cells at 20° C was unchanged, indicating that these cells were alive and functional, the process of intracellular dissolution of the phagocytized Co<sub>3</sub>O<sub>4</sub> particles did not continue at room temperature. Therefore, particle dissolution appears to be a highly sensitive function of AM metabolic state.

# Discussion

# Dissolution of 57Co<sub>3</sub>O<sub>4</sub> Particles In Vitro and In Vivo

The results just presented show that alveolar macrophages in vitro can dissolve particles that are insoluble in cell-free solutions. How do these data help us understand the kinetics of "insoluble" particle clearance in the lungs of living humans and animals?

Previous studies have demonstrated that the long-term clearance of monodisperse, porous  $\text{Co}_3\text{O}_4$  particles from the lungs could be largely attributed to dissolution processes resulting in Co translocation from the lungs to the blood (19, 22, 23, 32–34). That translocation rate decreased with increasing size (decreasing surface area) of the inhaled particles, similar to the decreasing *in vitro* dissolution rate. The particles were produced under similar conditions to those used in this study. For example, the 0.8- $\mu$ m particles used here came from the same batch as those used in the European interspecies comparison (22, 23, 32, 33).

In vivo pulmonary translocation rates during the first 2 wk after inhalation derived from lung retention measurements and excreta analysis in previous publications (19, 32) are listed in Table 6. Similarly, the human translocation rates (33) in Table 6 were derived from similar measurements and analyses carried out within the European interspecies comparison on lung clearance (22, 23, 32, 33).

In vitro dissolution rates (Table 4) can be compared to those in vivo rates given in Table 6 since both extracellular leaching and intracellular dissolution mechanisms are occurring in the lungs as well as in the in vitro tests. The in vivo and in vitro rates agree very well, especially the rates found in the lungs and in cultured AM for 0.3-, 0.8- and 1.7- $\mu$ m particles. Changes of the particle porosity and structure from batch to batch due to slight variations during aerosol production might have resulted in the differences seen between the in vivo and in vitro rate of 0.7- $\mu$ m particles.

### Dissolution Kinetics of 57Co<sub>3</sub>O<sub>4</sub> Particles

Models of dissolution need to consider both the physical and chemical properties of the particles and the cellular milieu that envelops them. Although the intracellular processes are complex, we were able to apply a relatively simple model to this system. This model applies to four different dissolution kinetics of four different-sized Co<sub>3</sub>O<sub>4</sub> particles. It de-

TABLE 2

Mean dissolved Co fractions of the initial particle mass in cell lysates\*

|         | Particle Size (µm) |                 |                 |               |
|---------|--------------------|-----------------|-----------------|---------------|
|         | 1.7                | 0.8             | 0.7             | 0.3           |
| Human 1 | $0.23 \pm 0.09$    | $0.73 \pm 0.38$ | $0.49 \pm 0.17$ | $8.0 \pm 1.8$ |
| Human 2 | $0.24\ \pm\ 0.01$  | ND              | $0.60\pm0.07$   | $7.1 \pm 1.4$ |
| Dog 1   | $0.23 \pm 0.17$    | ND              | $0.53 \pm 0.15$ | $4.9 \pm 0.5$ |
| Dog 2   | $0.30 \pm 0.18$    | ND              | $0.59 \pm 0.20$ | $6.4 \pm 3.4$ |
| Dog 3   | $0.16 \pm 0.04$    | $0.20 \pm 0.05$ | $0.34 \pm 0.08$ | $3.5 \pm 0.7$ |
| Dog 4   | $0.15 \pm 0.07$    | $0.54 \pm 0.25$ | $0.49 \pm 0.09$ | $3.4 \pm 0.7$ |
| Dog 5   | $0.17 \pm 0.09$    | $0.44 \pm 0.13$ | $0.41 \pm 0.19$ | $3.2 \pm 0.8$ |
| Dog 6   | $0.21 \pm 0.14$    | $0.40 \pm 0.11$ | $0.51 \pm 0.23$ | $3.1 \pm 1.1$ |
| Mean ±  |                    |                 |                 |               |
| SD      | $0.20\ \pm\ 0.13$  | $0.40\pm0.14$   | $0.48 \pm 0.17$ | $4.1 \pm 1.6$ |

ND = not determined.

scribes the dissolution of Co from the total surface area of these porous particles. Its parameters are the dissolution rate and the initial surface area. The mean dissolution rates remain constant within less than 10% for various periods during the 2 wk of incubation. A dissolution rate constant for Co<sub>3</sub>O<sub>4</sub> in the vacuolar environment of the AM was derived from measured particle parameters such as the initial geometric diameter, the density, and specific surface area.

The mean dissolution rate constant k is  $1.4 \pm 0.1 \times 10^{-8}$  g cm<sup>-2</sup> d<sup>-1</sup> for 0.7-, 0.8- and 1.7- $\mu$ m particles, as mentioned above; however, for 0.3- $\mu$ m particles, the rate constant is  $7.2 \times 10^{-8}$  g cm<sup>-2</sup> d<sup>-1</sup>. Obviously, there is a large difference between the 0.3- $\mu$ m particles and the larger particles. Inaccuracies in the sizing of these particles using a scanning electron microscope (SEM) could contribute to this error. If Equations 4 and 5 are used to calculate the ini-

TABLE 3
Standard deviation of three dissolution rates\*

| Particle Size (μm) |  |  |  |
|--------------------|--|--|--|
| 0.3                |  |  |  |
| 1 0.110            |  |  |  |
| 6 0.067            |  |  |  |
| 0 0.172            |  |  |  |
| 7 0.023            |  |  |  |
| 8 0.047            |  |  |  |
| 6 0.092            |  |  |  |
| 5 0.049            |  |  |  |
| 5 0.142            |  |  |  |
| 5                  |  |  |  |

ND = not determined.

TABLE 4
In vitro particle dissolution rates\*

|         | Particle Size (μm) |                 |                 |               |
|---------|--------------------|-----------------|-----------------|---------------|
|         | 1.7                | 0.8             | 0.7             | 0.3           |
| Human 1 | $0.17 \pm 0.05$    | $0.51 \pm 0.21$ | $0.36 \pm 0.09$ | $5.1 \pm 0.3$ |
| Human 2 | $0.15\pm0.03$      | ND              | $0.38\pm0.08$   | $4.0 \pm 0.9$ |
| Dog 1   | $0.20 \pm 0.03$    | ND              | $0.35 \pm 0.08$ | $3.5 \pm 0.3$ |
| Dog 2   | $0.20 \pm 0.03$    | ND              | $0.58 \pm 0.11$ | $8.6 \pm 1.4$ |
| Dog 3   | $0.22\ \pm\ 0.07$  | $0.37 \pm 0.12$ | $0.57 \pm 0.16$ | $5.9 \pm 0.5$ |
| Dog 4   | $0.21 \pm 0.07$    | $0.51 \pm 0.14$ | $0.47 \pm 0.12$ | $5.3 \pm 0.9$ |
| Dog 5   | $0.21 \pm 0.06$    | $0.47 \pm 0.14$ | $0.54 \pm 0.15$ | $5.5 \pm 0.6$ |
| Dog 6   | $0.17 \pm 0.06$    | $0.40 \pm 0.09$ | $0.40 \pm 0.05$ | $3.4 \pm 0.6$ |
| Mean ±  |                    |                 | _               | _             |
| SD      | $0.21\pm0.06$      | $0.45\pm0.23$   | $0.49 \pm 0.12$ | $5.4 \pm 1.1$ |

ND = not determined.

tial size of the small particles from the mean dissolution rate constant of the larger particles, 0.06  $\mu m$  instead of 0.3  $\mu m$  is obtained. For SEM analysis, particles are coated with a gold layer. The thickness of the gold coating might vary between 5 and 50 nm or more depending on the operating conditions of the coater used in this study. Thus, this cannot account for the difference seen. Hence, it is likely that the physical and chemical characteristics of these particles are sufficiently different (e.g., their surface-to-volume ratio) to result in a different rate constant for dissolution.

The dissolution of  ${}^{57}\text{Co}_3\text{O}_4$  particles outside a biologic system has been studied extensively (19–21, 32). Samples of 0.3-, 0.7-, and 1.7- $\mu$ m particles have been studied in saline at room temperature and at pH of 7.2 and 5.0 over a period of at least 70 d (19–21). An early leaching effect, the same as seen in our media-only studies, was observed in these saline studies. Dissolution after this initial leaching was less than

TABLE 5
Intracellular particle dissolution rates\*

|         | Particle Size (µm) |                 |                 |               |
|---------|--------------------|-----------------|-----------------|---------------|
|         | 1.7                | 0.8             | 0.7             | 0.3           |
| Human 1 | $0.13 \pm 0.03$    | $0.41 \pm 0.14$ | $0.28 \pm 0.05$ | 5.1 ± 0.3     |
| Human 2 | $0.12 \pm 0.02$    | ND              | $0.29\pm0.05$   | $3.4 \pm 0.7$ |
| Dog 1   | $0.16 \pm 0.02$    | ND              | $0.27 \pm 0.10$ | $2.7 \pm 0.6$ |
| Dog 2   | $0.17 \pm 0.03$    | ND              | $0.53 \pm 0.08$ | $8.1 \pm 1.2$ |
| Dog 3   | $0.17 \pm 0.04$    | $0.24 \pm 0.02$ | $0.43 \pm 0.06$ | $5.4 \pm 0.3$ |
| Dog 4   | $0.14 \pm 0.05$    | $0.38 \pm 0.09$ | $0.37 \pm 0.07$ | $4.5 \pm 0.6$ |
| Dog 5   | $0.16 \pm 0.03$    | $0.37 \pm 0.09$ | $0.46 \pm 0.13$ | $5.0 \pm 0.5$ |
| Dog 6   | $0.15 \pm 0.05$    | $0.33 \pm 0.06$ | $0.33 \pm 0.04$ | $3.0 \pm 0.6$ |
| Mean ±  |                    |                 |                 |               |
| SD _    | $0.16 \pm 0.04$    | $0.33 \pm 0.10$ | $0.40 \pm 0.09$ | $4.8 \pm 1.0$ |
|         |                    |                 |                 |               |

ND = not determined.

<sup>\*</sup> Since there is little change in the  $^{57}\text{Co}$  fractions in cell lysates over time (Figure 3), all data are presented as mean dissolved  $^{57}\text{Co}$  fractions in the filtered cell lysate (given as % of the initial  $^{57}\text{Co}_{:}\text{O}_{4}$  particle mass  $\pm$  SD) for four different particle sizes obtained from AM cultures from two human volunteers and six dogs. Canine fractions are averaged for each particle size and given as means and standard deviation.

<sup>\*</sup> Determined either from data over the whole period or without data from the first 6 d of incubation or without data after 10 d of incubation. Each standard deviation was normalized to its mean dissolution rate. Calculations were made for each particle size and all human and canine data sets.

<sup>\*</sup> In vitro dissolution rates (given as %/d of the initial  $^{57}\text{Co}_3\text{O}_4$  particle mass  $\pm$  SD) for four different particle sizes obtained from suspensions of cultured AM lavaged from two human volunteers and six dogs. Rates from dogs are averaged for each particle size and given as means  $\pm$  SD.

<sup>\*</sup> Intracellular dissolution rates (given as %/d of the initial  $^{57}\text{Co}_3\text{O}_4$  particle mass  $\pm$  SD) for four different particle sizes obtained from cultured AM lavaged from two human volunteers and six dogs. Extracellular particle leaching was subtracted prior to calculation. Rates from dogs are averaged for each particle size and given as means  $\pm$  SD.

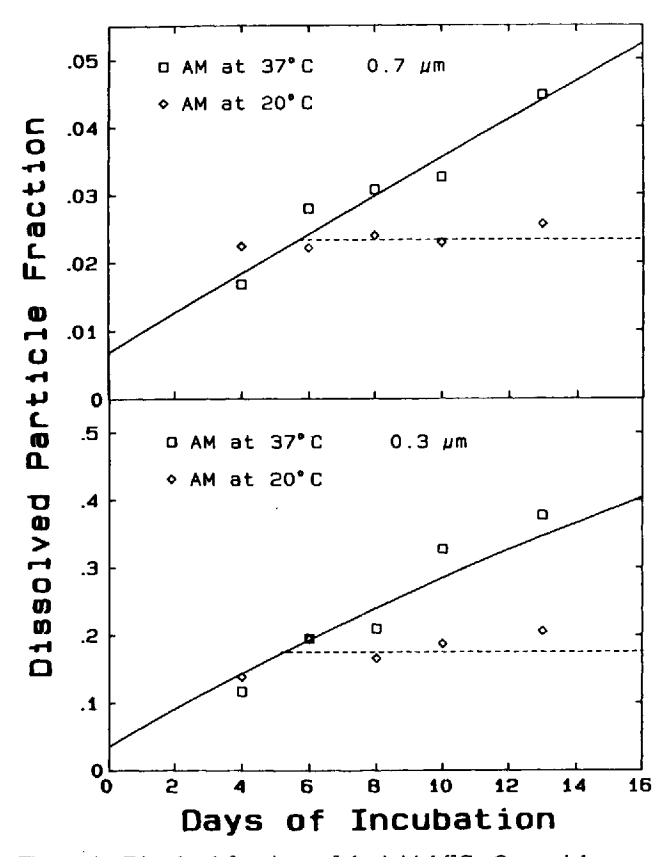


Figure 4. Dissolved fractions of the initial <sup>57</sup>Co<sub>3</sub>O<sub>4</sub> particle mass for 0.3- and 0.7-μm particles phagocytized in AM of dog 6 in two plates during 14 d of incubation. Incubation temperature was changed in one plate from 37° C to 20° C after 4 d of incubation. Note that the vertical scales differ for the two particle sizes.

0.07%/d of the particle mass. (Only  $0.3-\mu m$  particles at pH 5.0 were dissolved at a greater rate: 0.3%/d). In a 650-d study (32) on 0.8- and  $1.7-\mu m$  Co<sub>3</sub>O<sub>4</sub> particles, the dissolution rate was 0.002 and 0.001%/day, respectively, regardless of the pH value of the saline. In addition, particle dissolution in media alone at  $20^{\circ}$  C and  $37^{\circ}$  C incubation did not differ significantly for any of the particles used in this study. Using Equations 4 and 5, the dissolution rate constant for this saline study was  $10^{-9}$  g cm<sup>-2</sup> d<sup>-1</sup>, which is considerably smaller than the rate constant found for intracellular dissolution.

### Dissolution Properties of Aerosol Particles

In the literature (35), the dissolution rate constant in a lung fluid simulant was measured for only one other heavy metal oxide: CeO<sub>2</sub>, 7.6 × 10<sup>-8</sup> g cm<sup>-2</sup> d<sup>-1</sup>. This determination was based on a polydisperse aerosol with an unknown specific surface area. However, there are dissolution rate constants for a number of heavy metal oxides which were derived from linear kinetic models based on lung retention and clearance measurements of different-sized particles of one compound. For the most insoluble heavy metal oxides (6, 9–12, 14–17, 35, 36), these rate constants vary from 1 to 10 × 10<sup>-8</sup> g cm<sup>-2</sup> d<sup>-1</sup>. The intracellularly derived rate constant of <sup>57</sup>Co<sub>3</sub>O<sub>4</sub> particles used in this study is within this range. Because our

TABLE 6
In vivo particle dissolution rates\*

|        | Particle Size (µm)        |                              |                            |               |
|--------|---------------------------|------------------------------|----------------------------|---------------|
|        | 1.7                       | 0.8                          | 0.7                        | 0.3           |
| Human  | $0.14 \pm 0.02$           | $0.24 \pm 0.03$              |                            |               |
| rates  | $0.26\pm0.03$             | $0.34\ \pm\ 0.07$            |                            |               |
| Canine | $0.20 \pm 0.05$           | $0.40 \pm 0.06$ <sup>‡</sup> | $0.92 \pm 0.34^{\ddagger}$ | $8.2 \pm 1.3$ |
| rates  | $0.27 \pm 0.05^{\dagger}$ | $0.39 \pm 0.04$              | $1.45 \pm 0.26$            | $7.0 \pm 1.5$ |
|        | $0.25 \pm 0.05$           |                              | $1.27 \pm 0.06$            |               |
|        | $0.24 \pm 0.05$           |                              | $1.51 \pm 0.07$            |               |
|        | 0.27 + 0.11‡              |                              | _                          |               |
|        | $0.21 \pm 0.09$           |                              |                            |               |
| Mean ± |                           |                              |                            |               |
| SD     | $0.24 \pm 0.07$           | $0.40\pm0.05$                | $1.29\pm0.30$              | $7.6 \pm 1.4$ |

<sup>\*</sup> In vivo dissolution rates and SD (given as %/d of the initial particle mass) of  $^{57}\text{Co}_3\text{O}_4$  particles of four different sizes evaluated from published retention and excretion data of four human volunteers (22, 33) and 12 dogs (19, 22, 32) during the first 2 wk after inhalation. Rates from dogs are averaged for each particle size and given as means  $\pm$  SD. (Experiments marked with a dagger for 1.7- $\mu$ m particles were derived from two sequential studies on one dog; similarly, experiments marked with a double dagger for 0.7- $\mu$ m and 0.8- $\mu$ m particles were also derived from one dog.)

monodisperse particles are porous, we were able to make direct measurements to establish the dissolution rate constant rather than making indirect estimations from linear kinetic models.

In former studies (3, 4, 6, 7, 9–12, 14, 16, 17), in vivo dissolution rates of various metal compound aerosol particles were found to be similar to in vitro dissolution rates in solvents representing extracellular epithelial lining fluid. However, most of these polydisperse particle samples were nonporous and hence very insoluble with dissolution rates 1 to 2 orders of magnitude smaller than those test particles used in this study, resulting in larger errors caused by detection limits. Additionally, the translocation and metabolism of the dissolved particle mass from the lungs in the body was frequently more complicated than the simple translocation and metabolism of Co, such that in vivo translocation rates were estimated from lung retention curves. In order to obtain such an estimate, it was also necessary to assume certain rates for particle transport from the lung parenchyma to the gastrointestinal tract.

### Dissolution Rates in Cultured AM

In recent studies (24–29), the *in vitro* dissolution rates in cultured AM were found to be larger than those rates obtained from lung fluid simulants for cobalt, beryllium, manganese, arsenic compounds. For our monodisperse, homogeneous  ${}^{57}\text{Co}_3\text{O}_4$  particles, the dissolution patterns also appear to be completely different from lung fluid simulants. Deposited particles on the alveolar epithelium are usually phagocytized within the first day predominantly by AM (1, 37). When lungs were lavaged up to 500 d after exposure, more than 80% of the particles were associated with AM as was shown by autoradiography (34). Therefore, most particles on the epithelial surface are retained intracellularly in AM and are thus subject to those dissolution processes investigated in these cell culture studies. Hence, these cell culture studies

simulate the fate of particles in the lungs far more appropriately than do lung fluid simulant studies and represent a new approach to estimating solubilization of aerosols in the lungs.

An important factor for the difference in intracellular versus extracellular dissolution kinetics is the pH value of the vacuolar sol in which the particle is suspended. After it is entrapped inside a membrane-bound phagosome, lysosomes fuse and pour proteolytic enzymes and other digesting agents into the phagolysosome (39-42). Lysosome fusion also decreases the pH value from 7.2 to 4.5-5.5 in the phagolysosome (41, 42). However, although particle dissolution in saline at pH 5 increased slightly, the dissolution pattern still was not comparable to the intracellular dissolution shown here (19-21, 31, 32). Therefore, we suspect the interaction of co-factors such as chelators, enzymes, oxygen radicals, or other possible agents present in the phagolysosome.

From the constant dissolved fractions in the cell lysates at 4 to 16 d of incubation, a linear kinetic model was used to estimate the release of dissolved Co from the cells into the medium. This occurred in no less than 12 and no more than 24 h. Interestingly, fractions in the human AM are consistently higher than in canine AM, reflecting a somewhat slower transport of dissolved Co from the human cells.

#### **Human and Canine Dissolution Rates**

We only studied AM from two human volunteers. However, if we exclude the human dissolution rate for 0.8  $\mu$ m, which shows a large standard deviation, dissolution rates in human AM appear to be consistently smaller for each particle size when compared to the rates of canine AM (Table 5). This might reflect species differences in the intracellular particle dissolution of AM. A similar result of less effective translocation in human lungs rather than in canine lungs was found in the European interspecies comparison of lung clearance during more than 6 mo of observation (22, 23). More data are required to distinguish whether these differences account for interspecies or intersubject variability, particularly in humans. The uncertainty associated with extrapolating dissolution and translocation rates from dogs to humans should, however, be recognized.

# Conclusion

We have shown that particles are dissolved intracellularly in human and canine AM. Dissolution is proportional to the specific surface area of the particles in AM of both species and is well described by a dissolution rate derived from a simple model. The dissolution kinetics for a given particle is comparable in AM of both species. The *in vitro* dissolution rates determined in this study are similar to in vivo translocation rates found in previous long-term lung clearance studies in both humans and dogs. Therefore, this rather inexpensive and simple in vitro assay might be used to assess intracellular particle dissolution rates of new inhalable materials and thus predict their lung clearance kinetics in situ.

Acknowledgments: These studies were supported in part by Grants ES-00002, HL-31021, HL-27244 from the U.S. Public Health Service; by the US-FRG cooperative program in pulmonary research; and by the GSF F+E Vorhaben

#### References

- 1. Brain, J. D. 1985. Macrophages in the respiratory tract. In Handbook of Physiology. The Respiratory System I, Chapter 14. A. P. Fishman and A. B. Fisher, editors. American Physiological Society, Bethesda, MD.
- 2. Morrow, P. E., D. V. Bates, B. R. Fish, T. F. Hatch, and T. T. Mercer. 1966. ICRP Taskgroup on Lung Dynamics, 1966. Deposition and retention models for internal dosimetry of the human respiratory tract. Health Phys. 12:173-207
- 3. Morrow, P. E., F. R. Gibb, H. Davis, and M. Fisher. 1968. Dust removal from the lung parenchyma: an investigation of clearance simulants. Toxicol. Appl. Pharmacol. 12:372-396.
- 4. Morrow, P. E. 1973. Alveolar clearance of aerosols. Arch. Intern. Med. 131:101-108.
- 5. Mercer, T. T. 1967. On the role of particle size in the dissolution of lung burdens. Health Phys. 13:1211-1224.
- Kanapilly, G. M., O. G. Raabe, C. H. T. Goh, and R. A. Chimenti. 1973. Measurement of in vitro dissolution of aerosol particles for comparison to in vivo dissolution in the lower respiratory tract after inhalation. Health Phys. 24:497-507
- 7. Kanapilly, G. M. 1977. Alveolar microenvironment and its relationship to the retention and transport into blood of aerosols deposited in the alveoli. Health Phys. 32:89–100.
- 8. ICRP 30 International Commission on Radiological Protection. 1979. Units for intakes of radionuclides by workers. ICRP Publication 30, Annals of the ICRP. Pergamon Press, Oxford.
- McClellan, R. O., H. A. Boyd, A. F. Gallegos, and R. G. Thomas. 1972. Retention and distribution of <sup>244</sup>Cm following inhalation of <sup>244</sup>CmCl<sub>3</sub> and <sup>4</sup>CmO<sub>1.73</sub> by dogs. Health Phys. 22:877-885.
- 10. Cuddihy, R. G., and W. C. Griffith. 1972. A biological model describing tissue distribution and whole body retention of barium and lanthanum in beagle dogs after inhalation and gavage. Health Phys. 23:621-633.
- 11. Cuddihy, R. G., S. R. Gomez, and R. C. Pfleger. 1975. Inhalation exposures of beagle dogs to cerium aerosols: physical, chemical and mathematical analysis. Health Phys. 29:257-265
- 12. Cuddihy, R. G. 1982. Mathematical model for predicting clearance of inhaled radioactive materials. In Lung Modelling for Inhalation of Radioactive Materials. EUR 9384 EN. H. Smith and G. Gerber, editors. Commission of the European Communities, Brussels. 167-180,
- 13. Barnes, J. E., G. M. Kanapilly, and G. J. Newton, 1976. Cobalt-60 oxide aerosols: methods of production and short-term retention and distribution kinetics in the beagle dog. Health Phys. 30:391-398.
- 14. Moss, O. R. 1976. Dissolution of uranium and vanadium from aerodynamically size-separated ore particles in a simulated lung fluid. Ph.D. thesis. University of Rochester, Rochester.
- 15. Moss, O. R., and G. M. Kanapilly. 1980. Dissolution of inhaled aerosols. In Generation of Aerosols and Facilities for Exposure Experiments. K. Willeke, editor. Ann Arbor Science Publishers, Ann Arbor, MI. 105-124.
- Mewhinney, J. A., W. C. Griffith, and B. A. Muggenburg. 1982. The influ-ence of aerosol size on retention and translocation of <sup>241</sup>Am following inhalation of <sup>24</sup> AmO<sub>2</sub> by beagles. *Health Phys.* 42:611-628.

  17. Mewhinney, J. A., and W. C. Griffith. 1982. Models of Am metabolism in
- beagles and humans. Health Phys. 42:629-644
- 18. Kreyling, W. G., G. A. Ferron, and B. Haider. 1985. Total and regional lung retention of monodisperse cobalt compound aerosols after a single inhalation. Z. Erkr. Atmungsorgane 164:60–66.
- 19. Kreyling, W. G., G. A. Ferron, and B. Haider. 1986. Metabolic fate of cobalt aerosols in beagle dogs. Health Phys. 51:773-793.
- 20. Kreyling, W. G. 1983. Eine Methode zur Bestimmung der Retention nach Inhalation von Testaerosolen. GSF-Bericht S-936, Neuherberg-München.
- 21. Kreyling, W. G., and G. A. Ferron. 1984. Production of cobalt oxide aerosols with a modified spinning top aerosol generator. J. Aerosol Sci. 15: 367-371
- 22. Bailey, M. R., W. G. Kreyling, S. André et al. 1988. An interspecies comparison of the translocation of material from lung to blood. Ann. Occup. Hyg. 32:975-985
- 23. Bailey, M. R., W. G. Kreyling, S. André et al. 1989. An interspecies comparison of the lung clearance of inhaled monodisperse cobalt oxide particles. Part 1: objectives and summary of results. J. Aerosol Sci. 20:169-188.
- 24. Lundborg, M., B. Lind, and P. Camner. 1984. Ability of rabbit alveolar macrophages to dissolve metals. Exp. Lung Res. 7:11-22
- 25. Lundborg, M., A. Eklund, B. Lind, and P. Camner. 1985. Dissolution of metals by human and rabbit alveolar macrophages. Br. J. Ind. Med. 42: 642-655
- 26. Kreyling, W. G., G. A. Ferron, J. J. Godleski, B. Haider, and S. T. Kariya. 1986. The dissolution of monodisperse, porous cobaltosic oxide particles in the dog's lungs and in its alveolar macrophages. In Aerosols: Formation and Reactivity. W. Schikarski, H. J. Fissan, and S. K. Friedlander, editors. Pergamon Press, Oxford. 232-236.
- 27. Kreyling, W. G., J. J. Godleski, and J. D. Brain. 1987. A new functional parameter for alveolar macrophages: dissolution of inert test particles. EULEP Newsletter 45:57-64.

- Marafante, E., M. Lundborg, M. Vahter, and P. Camner. 1987. Dissolution of two arsenic compounds by rabbit alveolar macrophages in vitro. Fundam. Appl. Toxicol. 8:382–388.
- André, S., H. Métivier, G. Lantenois, M. Boyer, D. Nolibé, and R. Masse. 1987. Beryllium metal solubility in the lung, comparison of metal and hotpressed forms by in vivo and in vitro dissolution assays. *Hum. Toxicol*. 6:2330-2340.
- André, S., and H. Métivier. 1987. In vitro solubility of Co<sub>3</sub>O<sub>4</sub> particles using rat, baboon and human cultured alveolar macrophages. Comparison with in vitro acellular solubility and in vivo solubility. EULEP Newsletter 45:47-56.
- Kreyling, W. G., and G. A. Ferron. 1984. Physical and chemical analysis
  of cobalt oxide aerosol particles used for inhalation studies. *In Aerosols:*Science, Technology and Industrial Applications of Airborne Particles.
  B. Y. H. Liu, D. Y. H. Pui, and H. Fissan, editors. Elsevier, New York.
  985-989.
- Kreyling, W. G., G. A. Ferron, and B. Haider. 1989. Part 4: lung clearance of inhaled cobalt oxide in beagle dogs. J. Aerosol Sci. 20:219-232.
- Foster, P. P., I. Pearman, and D. Ramsden. 1989. Part 2: lung clearance of inhaled cobalt oxide in man. J. Aerosol Sci. 20:189-201.
- Kreyling, W. G., G. Schumann, A. Ortmaier, G. A. Ferron, and E. Karg. 1988. Particle transport from the lower resporatory tract. J. Aerosol Med. 1:351–370.

- Kanapilly, G. M., and C. H. T. Goh. 1973. Some factors affecting the in vitro rates of dissolution of respirable particles of relatively low solubility. Health Phys 25:255-237.
- Mewhinney, J. A., and J. H. Diehl. 1983. Retention of inhaled <sup>238</sup>PuO in beagles: a mechanistic approach to description. *Health Phys.* 45:39–60
- Sorokin, S. P., and J. D. Brain. 1975. Pathways of clearance in mouse lungs exposed to iron oxide aerosols. *Anat Rec.* 181:581-626.
- Rebar, A. H., D. B. DeNicola, and B. A. Muggenberg. 1980. Bronchopulmonary lavage cytology in the dog: normal findings. Vet. Pathol. 12: 294-304.
- Geisow, M. J., P. D'Arcy Hart, and M. R. Young. 1981. Temporal changes of lysosome and phagosome pH during phagolysosome formation in macrophages: studies by fluorescence spectroscopy. J. Cell Biol. 89:645–652.
- Geisow, M. J. 1984. Fluorescein conjugates as indicators of subcellular pH. A critical evaluation. Exp. Cell Res. 150:29-35.
- Nilsen, A., K. Nyberg, and P. Camner. 1988. Intraphagosomal pH in alveolar macrophages after phagocytosis in vivo and in vitro of fluoresceinlabeled yeast particles. Exp. Lung Res. 14:197-207.
- Nyberg, K., A. Johannson, and P. Camner. 1989. Intraphagosomal pH in alveolar macrophages studied with fluorescein-labelled amorphous silica particles. Exp. Lung Res. 15:49-62.